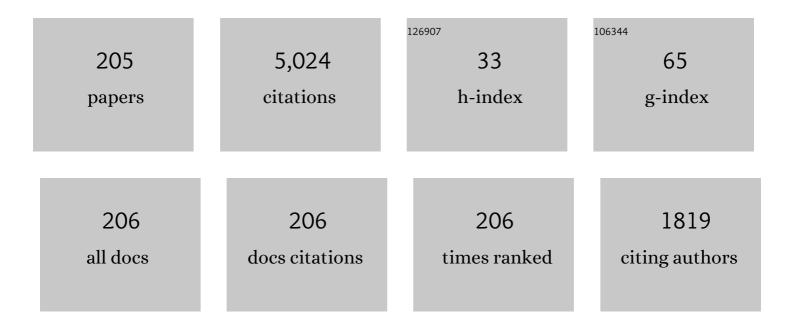
List of Publications by Year in descending order

Source: https://exaly.com/author-pdf/1353516/publications.pdf Version: 2024-02-01



#	Article	IF	CITATIONS
1	Formation process of tungsten nanostructure by the exposure to helium plasma under fusion relevant plasma conditions. Nuclear Fusion, 2009, 49, 095005.	3.5	494
2	Formation of Nanostructured Tungsten with Arborescent Shape due to Helium Plasma Irradiation. Plasma and Fusion Research, 2006, 1, 051-051.	0.7	375
3	TEM observation of the growth process of helium nanobubbles on tungsten: Nanostructure formation mechanism. Journal of Nuclear Materials, 2011, 418, 152-158.	2.7	226
4	On the Acoustic Nonlinearity of Solid-Solid Contact With Pressure-Dependent Interface Stiffness. Journal of Applied Mechanics, Transactions ASME, 2004, 71, 508-515.	2.2	189
5	Static and dynamic behaviour of plasma detachment in the divertor simulator experiment NAGDIS-II. Nuclear Fusion, 2001, 41, 1055-1065.	3.5	185
6	Sub-ms laser pulse irradiation on tungsten target damaged by exposure to helium plasma. Nuclear Fusion, 2007, 47, 1358-1366.	3.5	180
7	Experimental Evidence of Molecular Activated Recombination in Detached Recombining Plasmas. Physical Review Letters, 1998, 81, 818-821.	7.8	130
8	Space-Charge Limited Current from Plasma-Facing Material Surface. Contributions To Plasma Physics, 2004, 44, 126-137.	1.1	123
9	Extension of the operational regime of the LHD towards a deuterium experiment. Nuclear Fusion, 2017, 57, 102023.	3.5	116
10	Prompt ignition of a unipolar arc on helium irradiated tungsten. Nuclear Fusion, 2009, 49, 032002.	3.5	105
11	Helium plasma implantation on metals: Nanostructure formation and visible-light photocatalytic response. Journal of Applied Physics, 2013, 113, .	2.5	88
12	Influence of crystal orientation on damages of tungsten exposed to helium plasma. Journal of Nuclear Materials, 2013, 438, S879-S882.	2.7	87
13	Helium effects on tungsten surface morphology and deuterium retention. Journal of Nuclear Materials, 2013, 442, S267-S272.	2.7	83
14	Plasma detachment in linear devices. Plasma Physics and Controlled Fusion, 2017, 59, 034007.	2.1	80
15	Nanostructured Black Metal: Novel Fabrication Method by Use of Self-Growing Helium Bubbles. Applied Physics Express, 2010, 3, 085204.	2.4	77
16	Exfoliation of the tungsten fibreform nanostructure by unipolar arcing in the LHD divertor plasma. Nuclear Fusion, 2011, 51, 102001.	3.5	73
17	Thermal response of nanostructured tungsten. Nuclear Fusion, 2014, 54, 033005.	3.5	66
18	Studies of power exhaust and divertor design for a 1.5 GW-level fusion power DEMO. Nuclear Fusion, 2017, 57, 126050.	3.5	65

#	Article	IF	CITATIONS
19	Enhanced growth of large-scale nanostructures with metallic ion precipitation in helium plasmas. Scientific Reports, 2018, 8, 56.	3.3	60
20	Growth of multifractal tungsten nanostructure by He bubble induced directional swelling. New Journal of Physics, 2015, 17, 043038.	2.9	57
21	In situ observation of structural change of nanostructured tungsten during annealing. Journal of Nuclear Materials, 2014, 449, 9-14.	2.7	56
22	Confinement and structure of electrostatically coupled dust clouds in a direct current plasma–sheath. Physics of Plasmas, 1998, 5, 3517-3523.	1.9	48
23	Hybrid simulation research on formation mechanism of tungsten nanostructure induced by helium plasma irradiation. Journal of Nuclear Materials, 2015, 463, 109-115.	2.7	48
24	Measurement of heat diffusion across fuzzy tungsten layer. Results in Physics, 2016, 6, 877-878.	4.1	48
25	Fuzzy nanostructure growth on Ta/Fe by He plasma irradiation. Scientific Reports, 2016, 6, 30380.	3.3	47
26	Heat flows through plasma sheaths. Physics of Plasmas, 1998, 5, 2151-2158.	1.9	44
27	Arcing on tungsten subjected to helium and transients: ignition conditions and erosion rates. Plasma Physics and Controlled Fusion, 2012, 54, 035009.	2.1	44
28	Growth annealing equilibrium of tungsten nanostructures by helium plasma irradiation in non-eroding regimes. Journal of Nuclear Materials, 2013, 440, 55-62.	2.7	44
29	Impact of arcing on carbon and tungsten: from the observations in JT-60U, LHD and NAGDIS-II. Nuclear Fusion, 2013, 53, 053013.	3.5	41
30	Surface modification of titanium using He plasma. Applied Surface Science, 2014, 303, 438-445.	6.1	41
31	Growth of nano-tendril bundles on tungsten with impurity-rich He plasmas. Nuclear Fusion, 2018, 58, 096022.	3.5	40
32	Influence of Plasma Resistance and Fluctuation on Probe Characteristics in Detached Recombining Plasmas. Contributions To Plasma Physics, 2001, 41, 473-480.	1.1	37
33	Reduction of laser power threshold for melting tungsten due to subsurface helium holes. Journal of Applied Physics, 2006, 100, 103304.	2.5	37
34	2D Statistical Analysis of Nonâ€Ðiffusive Transport under Attached and Detached Plasma Conditions of the Linear Divertor Simulator. Contributions To Plasma Physics, 2010, 50, 256-266.	1.1	34
35	Anomaly of Langmuir Probe Characteristics in Detached Recombining Plasmas. Contributions To Plasma Physics, 1998, 38, 31-37.	1.1	33
36	Visualized Blow-off from Helium Irradiated Tungsten in Response to ELM-like Heat Load. Plasma and Fusion Research, 2009, 4, 004-004.	0.7	33

#	Article	IF	CITATIONS
37	Field emission property of nanostructured tungsten formed by helium plasma irradiation. Fusion Engineering and Design, 2013, 88, 2842-2847.	1.9	33
38	Comparison of Damages on Tungsten Surface Exposed to Noble Gas Plasmas. Plasma Science and Technology, 2013, 15, 282-286.	1.5	33
39	Field Emission From Metal Surfaces Irradiated With Helium Plasmas. IEEE Transactions on Plasma Science, 2017, 45, 2080-2086.	1.3	33
40	Molecular activated recombination in divertor simulation plasma on GAMMA 10/PDX. Nuclear Materials and Energy, 2017, 12, 1004-1009.	1.3	32
41	Fuzzy nanostructure growth on precious metals by He plasma irradiation. Surface and Coatings Technology, 2018, 340, 86-92.	4.8	31
42	Transition from electrostatic-to-electromagnetic mode in a radio-frequency Ar inductively coupled plasma in atmospheric pressure. Journal of Applied Physics, 2004, 95, 427-433.	2.5	29
43	Tritium retention in nanostructured tungsten with large effective surface area. Journal of Nuclear Materials, 2013, 438, S1142-S1145.	2.7	29
44	Nonlinear interactions between high heat flux plasma and electronâ€emissive hot material surface. Physics of Plasmas, 1996, 3, 281-292.	1.9	28
45	Reconstruction of Velocity Distribution of Density Bursts by Wavelet Analysis in the Linear Divertor Simulator NAGDIS-II. Contributions To Plasma Physics, 2004, 44, 222-227.	1.1	28
46	Enhancement of cross-field transport into the private region of detached-divertor in Large Helical Device. Physics of Plasmas, 2010, 17, 102509.	1.9	27
47	Transition in velocity and grouping of arc spot on different nanostructured tungsten electrodes. Results in Physics, 2014, 4, 33-39.	4.1	27
48	Erosion of nanostructured tungsten by laser ablation, sputtering and arcing. Nuclear Materials and Energy, 2017, 12, 386-391.	1.3	26
49	Deepening of Floating Potential for Tungsten Target Plate on the way to Nanostructure Formation. Plasma and Fusion Research, 2010, 5, 039-039.	0.7	25
50	Helium plasma irradiation on single crystal tungsten and undersized atom doped tungsten alloys. Physica Scripta, 2014, 89, 025602.	2.5	25
51	Visualization of Intermittent Blobby Plasma Transport in Attached and Detached Plasmas of the NAGDIS-II. Journal of Plasma and Fusion Research, 2004, 80, 275-276.	0.4	24
52	Direct observation of cathode spot grouping using nanostructured electrode. Physics Letters, Section A: General, Atomic and Solid State Physics, 2009, 373, 4273-4277.	2.1	24
53	Formation and decay processes of Ar/He microwave plasma jet at atmospheric gas pressure. Journal of Applied Physics, 2011, 110, .	2.5	24
54	Motion of unipolar arc spots ignited on a nanostructured tungsten surface. Plasma Physics and Controlled Fusion, 2011, 53, 074002.	2.1	24

#	Article	IF	CITATIONS
55	Fractality of self-grown nanostructured tungsten by He plasma irradiation. Physics Letters, Section A: General, Atomic and Solid State Physics, 2014, 378, 2533-2538.	2.1	24
56	Sulfur K-edge XANES for methylene blue in photocatalytic reaction over WO3 nanomaterials. Nuclear Instruments & Methods in Physics Research B, 2015, 365, 35-38.	1.4	23
57	lgnition and erosion of materials by arcing in fusionâ€relevant conditions. Contributions To Plasma Physics, 2018, 58, 608-615.	1.1	23
58	Investigation of recombination front region in detached plasmas in a linear divertor plasma simulator. Nuclear Materials and Energy, 2019, 19, 458-462.	1.3	23
59	Morphologies of co-depositing W layer formed during He plasma irradiation. Nuclear Fusion, 2018, 58, 106002.	3.5	22
60	Formation Condition of Fiberform Nanostructured Tungsten by Helium Plasma Exposure. Plasma and Fusion Research, 2010, 5, S1023-S1023.	0.7	21
61	Investigation of arcing on fiber-formed nanostructured tungsten by pulsed plasma during steady state plasma irradiation. Fusion Engineering and Design, 2016, 112, 156-161.	1.9	21
62	Fabrication of photocatalytically active vanadium oxide nanostructures via plasma route. Journal Physics D: Applied Physics, 2018, 51, 215201.	2.8	20
63	Behavior of 23S metastable state He atoms in low-temperature recombining plasmas. Physics of Plasmas, 2017, 24, 073301.	1.9	19
64	Helium line emission spectroscopy in recombining detached plasmas. Physics of Plasmas, 2018, 25, 063303.	1.9	18
65	Localized spiraling plasma ejection contributing the ion-flux broadening in the detached linear plasma. Plasma Physics and Controlled Fusion, 2018, 60, 075013.	2.1	18
66	Accelerated/reduced growth of tungsten fuzz by deposition of metals. Journal of Nuclear Materials, 2021, 548, 152844.	2.7	18
67	Suppression of secondary electron emission from the material surfaces with grazing incident magnetic field in the plasma. Physics of Plasmas, 1996, 3, 4310-4312.	1.9	17
68	Statistical Analysis of the Spatial Behavior of Plasma Blobs Around the Plasma Column in a Linear Plasma Device. Contributions To Plasma Physics, 2012, 52, 424-428.	1.1	17
69	Fractality and growth of He bubbles in metals. Physics Letters, Section A: General, Atomic and Solid State Physics, 2017, 381, 2355-2362.	2.1	17
70	Field Emission From Nanostructured Tendril Bundles. IEEE Transactions on Plasma Science, 2019, 47, 5186-5190.	1.3	17
71	Numerical Simulation Study on Density Dependence of Plasma Detachment in Simulated Gas Divertor Experiments of The TPDâ€I Device. Contributions To Plasma Physics, 1996, 36, 339-343.	1.1	15
72	Power Transmission Factor for Tungsten Target w/wo Fiber-Form Nanostructure in He Plasmas with Hot Electron Component Using Compact Plasma Device AIT-PID. Fusion Science and Technology, 2013, 63, 225-228.	1.1	15

#	Article	IF	CITATIONS
73	A plasma source driven predator-prey like mechanism as a potential cause of spiraling intermittencies in linear plasma devices. Physics of Plasmas, 2014, 21, 032302.	1.9	15
74	Helium-plasma–induced straight nanofiber growth on HCP metals. Acta Materialia, 2019, 181, 342-351.	7.9	15
75	Tungsten fuzz: Deposition effects and influence to fusion devices. Nuclear Materials and Energy, 2020, 25, 100828.	1.3	15
76	Particle in Cell Simulation on Thermoelectron Emission from Hot Target Plate. Contributions To Plasma Physics, 1996, 36, 386-390.	1.1	14
77	Self-Affine Fractality of Bifurcating Arc Trail in Magnetized Plasma. Journal of the Physical Society of Japan, 2010, 79, 054501.	1.6	14
78	Influence of heavier impurity deposition on surface morphology development and sputtering behavior explored in multiple linear plasma devices. Nuclear Materials and Energy, 2019, 18, 67-71.	1.3	14
79	Proposal of Modified Child-Langmuir Formula describing Space-Charge Limited Current in Plasma. Contributions To Plasma Physics, 2004, 44, 144-149.	1.1	13
80	Ray tracing simulation for radiation trapping of the He I resonance transitions in a linear plasma device. Physics of Plasmas, 2009, 16, .	1.9	13
81	Flattening-induced electronic changes in zigzag single- and multi-walled boron nitride nanotubes: A first-principles DFT study. Physical Review B, 2009, 80, .	3.2	12
82	2D Measurement of Edge Plasma Dynamics by Using Highâ€ <b>S</b> peed Camera Based on Hel Line Intensity Ratio Method. Contributions To Plasma Physics, 2010, 50, 962-969.	1.1	12
83	Application of Nanostructured Tungsten Fabricated by Helium Plasma Irradiation for Photoinduced Decolorization of Methylene Blue. E-Journal of Surface Science and Nanotechnology, 2014, 12, 343-348.	0.4	12
84	Development of Nanostructured Black Metal by Self-Growing Helium Bubbles for Optical Application. Japanese Journal of Applied Physics, 2011, 50, 08JG01.	1.5	11
85	Spectroscopic Study and Motion Analysis of Arc Spot Initiated on Nanostructured Tungsten. Japanese Journal of Applied Physics, 2013, 52, 11NC02.	1.5	11
86	Photon Trapping Effects in DEMO Divertor Plasma. Contributions To Plasma Physics, 2016, 56, 657-662.	1.1	11
87	One‣tep Plasma Synthesis of Nb <sub>2</sub> O <sub>5</sub> Nanofibers and their Enhanced Photocatalytic activity. ChemPhysChem, 2018, 19, 3237-3246.	2.1	11
88	Effect of the Nanostructured Layer Thickness on the Dynamics of Cathode Spots on Tungsten. IEEE Transactions on Plasma Science, 2018, 46, 4044-4050.	1.3	11
89	Behavior of Plasma Response Field in Detached Plasma. Plasma and Fusion Research, 2013, 8, 1402058-1402058.	0.7	11
90	Increase in the work function of W/WO <sub>3</sub> by helium plasma irradiation. Japanese Journal of Applied Physics, 2015, 54, 126201.	1.5	10

#	Article	IF	CITATIONS
91	Transverse motion of a plasma column in a sheet plasma. Contributions To Plasma Physics, 2017, 57, 87-93.	1.1	10
92	Fabrication of a nanostructured TiO <sub>2</sub> photocatalyst using He plasma-irradiated tungsten and ethylene gas decomposition. Japanese Journal of Applied Physics, 2019, 58, SEEG01.	1.5	10
93	Detached helium plasma simulation by a one-dimensional fluid code with detailed collisional-radiative model. Physics of Plasmas, 2020, 27, 102505.	1.9	10
94	Photoelectrochemical properties of plasma-induced nanostructured tungsten oxide. Applied Surface Science, 2022, 580, 151979.	6.1	10
95	Title is missing!. Journal of Materials Science, 2001, 36, 5169-5175.	3.7	9
96	Ignition and Behavior of Arc Spots on Helium Irradiated Tungsten Under Fusion Relevant Condition. IEEE Transactions on Plasma Science, 2019, 47, 3609-3616.	1.3	9
97	Ignition and Sustainment of Arcing on Nanostructured Tungsten Under Plasma Exposure. IEEE Transactions on Plasma Science, 2019, 47, 3617-3625.	1.3	9
98	Spatiotemporal dynamics of cross-field ejection events in recombining detached plasma. Plasma Physics and Controlled Fusion, 2020, 62, 075011.	2.1	9
99	Enhanced photocatalytic ethylene decomposition with anatase-rutile mixed nanostructures formed by He plasma treatment. Journal of Photochemistry and Photobiology A: Chemistry, 2021, 418, 113420.	3.9	9
100	Numerical Simulation on Structure of Detached Helium Plasmas with Hydrogen and Helium Gas Puff in NAGDISâ€II. Contributions To Plasma Physics, 1998, 38, 55-60.	1.1	8
101	2-D PIC Simulation on Space-Charge Limited Emission Current from Plasma-Facing Components. Contributions To Plasma Physics, 2000, 40, 478-483.	1.1	8
102	Development of a Compact Divertor Plasma Simulator for Plasma-Wall Interaction Studies on Neutron-Irradiated Materials. Plasma and Fusion Research, 2017, 12, 1405040-1405040.	0.7	8
103	Localized Density Fluctuation in the Downstream of Detached Plasma. Plasma and Fusion Research, 2017, 12, 1202007-1202007.	0.7	8
104	Study of Plasma Current Decay in the Initial Phase of High Poloidal Beta Disruptions in JT-60U. Plasma and Fusion Research, 2011, 6, 1302136-1302136.	0.7	8
105	Observation of Arc Spots Initiated on Nanostructured Tungsten. IEEE Transactions on Plasma Science, 2013, 41, 1889-1895.	1.3	7
106	Enhancement of photocatalytic activity of TiO <sub>2</sub> by plasma irradiation. Japanese Journal of Applied Physics, 2016, 55, 106202.	1.5	7
107	Photocatalytic decomposition of ethylene using He plasma induced nano-TiO <sub>2</sub> . Japanese Journal of Applied Physics, 2019, 58, 070903.	1.5	7
108	Spatial and temporal measurement of recombining detached plasmas by laser Thomson scattering. Plasma Sources Science and Technology, 2019, 28, 105015.	3.1	7

#	Article	IF	CITATIONS
109	The influence of impurities on the formation of nanocone structures on silicon surface irradiated by low energy helium plasma. Journal of Applied Physics, 2020, 128, .	2.5	7
110	Application of dynamic mode decomposition to rotating structures in detached linear plasmas. Physics of Plasmas, 2020, 27, .	1.9	7
111	Fabrication of nanostructured Ti thin film with Ti deposition in He plasmas. Japanese Journal of Applied Physics, 2021, 60, 038004.	1.5	7
112	Computer Tomography on Divertor Impurity Monitor for ITER with Minimizing Errors in a Logarithmic Scale. Plasma and Fusion Research, 2021, 16, 2405019-2405019.	0.7	7
113	Unipolar arc plasmas on nanostructured tungsten surfaces under perpendicular magnetic field. Plasma Sources Science and Technology, 2020, 29, 125015.	3.1	7
114	Development of steady/transient dual plasma irradiation device using a plasma gun. Journal of Nuclear Materials, 2013, 438, S707-S710.	2.7	6
115	Tailoring of fuzzy nanostructures on porous tungsten skeleton by helium plasma irradiation. Japanese Journal of Applied Physics, 2017, 56, 030303.	1.5	6
116	Pulsation Effects of Incident Ion Energy on W Fuzz Growth. Plasma and Fusion Research, 2018, 13, 1205001-1205001.	0.7	6
117	Thomson Scattering Measurement of Two Electron Temperature Components in Transition to Detached Plasmas. Plasma and Fusion Research, 2018, 13, 1201099-1201099.	0.7	6
118	Helium-W co-deposition layer: TEM observation and D retention. Journal of Nuclear Materials, 2020, 540, 152350.	2.7	6
119	The dependence of Mo ratio on the formation of uniform black silicon by helium plasma irradiation. Journal Physics D: Applied Physics, 2021, 54, 405202.	2.8	6
120	Blob/Hole Generation in the Divertor Leg of the Large Helical Device. Plasma and Fusion Research, 2012, 7, 1402152-1402152.	0.7	6
121	Changes in morphology and field emission property of nano-tendril bundles after high temperature annealing. Nuclear Materials and Energy, 2022, 31, 101178.	1.3	6
122	Recent Results in Divertor Plasma Simulators. Journal of Plasma and Fusion Research, 2004, 80, 212-216.	0.4	5
123	Influence of expanding and contracting magnetic field configurations on detached plasma formation in a linear plasma device. Physics of Plasmas, 2017, 24, .	1.9	5
124	Development of Thomson Scattering Measurement System for Upstream Plasmas in the NAGDIS-II Device. Plasma and Fusion Research, 2019, 14, 2405031-2405031.	0.7	5
125	Doubleâ€probe measurement in recombining plasma using NAGDISâ€II. Contributions To Plasma Physics, 2019, 59, e201800088.	1.1	5
126	Multipoint measurements employing a microwave interferometer and a Langmuir probe in the detached linear plasma. AIP Advances, 2019, 9, 015016.	1.3	5

#	Article	IF	CITATIONS
127	Photocatalytic application of helium plasma induced nanostructured tungsten oxides. Japanese Journal of Applied Physics, 2020, 59, SAAB04.	1.5	5
128	Effect of temperature and incident ion energy on nanostructure formation on silicon exposed to helium plasma. Plasma Processes and Polymers, 2020, 17, 2000126.	3.0	5
129	Inspection of Arc Trails Formed in Stellarator/Heliotron Devices W7-X and LHD. Plasma and Fusion Research, 2020, 15, 2402012-2402012.	0.7	5
130	Microstructure and Retention in He-W Co-Deposition Layer. Plasma and Fusion Research, 2020, 15, 1201004-1201004.	0.7	5
131	Nano-tendril bundles behavior under plasma-relevant electric fields. Vacuum, 2021, 183, 109799.	3.5	5
132	Enhancement of Arc Ignition on Tungsten in Helium Plasmas with Impurity Gases. Plasma and Fusion Research, 2021, 16, 2405069-2405069.	0.7	5
133	Fluid Mechanical Characteristics of Microwave Discharge Jet Plasmas at Atmospheric Gas Pressure. IEEJ Transactions on Fundamentals and Materials, 2010, 130, 493-500.	0.2	5
134	Application of Ion Sensitive Probe to High Density Plasmas in Magnum-PSI. Plasma and Fusion Research, 2019, 14, 1202135-1202135.	0.7	5
135	Thin film and noble metal loading effects on the photocatalytic reactivity of helium-plasma-induced nanostructured tungsten oxides. Materials Research Express, 2020, 7, 075007.	1.6	5
136	Enhancement of Plasma Heat Flow to the Conductive Divertor Plate Associated with Crossâ€Field Potential Variation and Thermoelectron Emission. Contributions To Plasma Physics, 1998, 38, 349-354.	1.1	4
137	Low-energy helium irradiation on in-vessel mirror materials. Journal of Nuclear Materials, 2013, 442, S515-S519.	2.7	4
138	Strong Reduction of Ion Flux to a Target Plate in a Magnetically Contracting Detached Plasma. Plasma and Fusion Research, 2016, 11, 1202005-1202005.	0.7	4
139	Statistical Analysis of Particle Flux Flowing into the Endâ€Target in between Attached and Detached States in the Linear Divertor Plasma Simulator NAGDISâ€II. Contributions To Plasma Physics, 2016, 56, 723-728.	1.1	4
140	Measurement of He neutral temperature in detached plasmas using laser absorption spectroscopy. AIP Advances, 2018, 8, .	1.3	4
141	Blob- and hole-like structures outstanding during the transition from attached to detached divertor states in GAMMA 10/PDX. Physics of Plasmas, 2018, 25, 082505.	1.9	4
142	Influence of Nitrogen Ratio on Plasma Detachment during Combined Seeding with Hydrogen on Divertor Simulation Experiment of GAMMA 10/PDX. Plasma and Fusion Research, 2021, 16, 2402041-2402041.	0.7	4
143	Measurement of the Bidirectional Reflectance Distribution Function of Tungsten Surface Sputtered in Argon Plasma. Plasma and Fusion Research, 2022, 17, 2405041-2405041.	0.7	4
144	Simulation and experiment on detached plasmas in the linear divertor simulator NAGDIS-II. European Physical Journal D, 1998, 48, 127-136.	0.4	3

#	Article	IF	CITATIONS
145	Analysis of Detached Recombining Plasmas by Collisional-Radiative Model with Energetic Electron Component. Contributions To Plasma Physics, 2002, 42, 419-424.	1.1	3
146	Influence of Plasma-Neutral Collisions on Probe Measurements in Atmospheric Pressure Plasmas. Contributions To Plasma Physics, 2014, 54, 304-307.	1.1	3
147	Current Activities in the Interactive Joint Research at Tohoku University - Advanced Evaluation of Radiation Effects on Fusion Materials Plasma and Fusion Research, 2014, 9, 3405136-3405136.	0.7	3
148	Mode Structure Analysis of Detached Plasmas with 2D Images. Plasma and Fusion Research, 2018, 13, 1402033-1402033.	0.7	3
149	Generation of Spiral Shape Nitrogen Recombining Plasma for Atomic Nitrogen Source. Plasma and Fusion Research, 2019, 14, 3401069-3401069.	0.7	3
150	Dust Formation from Arc Spots on Nanostructured Tungsten Surface. Plasma and Fusion Research, 2020, 15, 1205061-1205061.	0.7	3
151	Dynamics of Hydrogen Isotope Absorption and Emission of Neutron-Irradiated Tungsten. Plasma and Fusion Research, 2020, 15, 1505081-1505081.	0.7	3
152	Particle simulation on multiple dust layers of Coulomb cloud in cathode sheath edge. European Physical Journal D, 1998, 48, 239-244.	0.4	2
153	Intermittent Structures in the High Field Side Boundary of the HYBTOK-II Tokamak. European Physical Journal D, 2003, 53, 863-868.	0.4	2
154	Formation and mitigation of fiberform nanostructured tungsten by helium and sub-ms laser pulse irradiations. Plasma Devices and Operations, 2009, 17, 165-173.	0.6	2
155	Conditions for the Release of a Metallic Dust Particle from a Plasma-Facing Wall. Contributions To Plasma Physics, 2012, 52, 478-483.	1.1	2
156	Effect of resistivity profile on current decay time of initial phase of current quench in neon-gas-puff inducing disruptions of JT-60U. Physics of Plasmas, 2013, 20, 112507.	1.9	2
157	Morphology and Optical Property Changes of Nanostructured Tungsten in LHD. Plasma and Fusion Research, 2015, 10, 1402083-1402083.	0.7	2
158	Modeling of Linear Divertor Plasma Simulator Experiments with Threeâ€dimensional Target Structure by Using EMC3â€EIRENE Code. Contributions To Plasma Physics, 2016, 56, 598-603.	1.1	2
159	Vacuum breakdown from nanostructured fuzzy surfaces. , 2016, , .		2
160	Detailed Analysis of Plasma Resistivity in Detached Recombining Plasmas. Contributions To Plasma Physics, 2016, 56, 717-722.	1.1	2
161	Size distribution of nano-tendril bundles with various additional impurity gases. Nuclear Materials and Energy, 2020, 25, 100843.	1.3	2
162	Modeling of the impurity-induced silicon nanocone growth by low energy helium plasma irradiation. Plasma Science and Technology, 2021, 23, 045503.	1.5	2

#	Article	IF	CITATIONS
163	Tungsten Large-Scale Fiberform Nanostructures Retained under High Temperature Conditions. Plasma and Fusion Research, 2021, 16, 1206001-1206001.	0.7	2
164	Fluctuation Characteristics in Detached Recombining Plasmas Journal of Plasma and Fusion Research, 2002, 78, 1093-1101.	0.4	2
165	Thermionic Energy Converter System Using Heat Flux in Divertor Region. Plasma and Fusion Research, 2012, 7, 1405050-1405050.	0.7	2
166	Fatal Damages due to Breakdown on a Diagnostic Mirror Located outside the Vacuum Vessel in JT-60U. Plasma and Fusion Research, 2012, 7, 2405121-2405121.	0.7	2
167	Nanostructure Growth on Rhodium/Ruthenium by the Exposure to He Plasma. Plasma and Fusion Research, 2018, 13, 3406065-3406065.	0.7	2
168	Spatiotemporal Structure of Hα Emission from the Detached Plasma in GAMMA 10/PDX. Plasma and Fusion Research, 2019, 14, 2402036-2402036.	0.7	2
169	Growth of Mo Large-Scale Fiberform Nanostructures. Plasma and Fusion Research, 2021, 16, 1206105-1206105.	0.7	2
170	Prospect on the Atomic and Molecular Processes in Plasmas 5. Recent Topics in Experiments 5.1 Molecular Activated Recombination Processes in Divertor Plasmas. Journal of Plasma and Fusion Research, 1999, 75, 1162-1168.	0.4	1
171	COMPUTATIONAL MODELING OF WAVE SCATTERING IN FIBER REINFORCED COMPOSITE MATERIALS. , 2002, , .		1
172	Sound Wave Propagation in Gases at Low Pressure. AIP Conference Proceedings, 2003, , .	0.4	1
173	Development of Divertor Plasma Simulators with High Heat Flux Plasmas and its Application to Nuclear Fusion Study: A Review. IEEJ Transactions on Electrical and Electronic Engineering, 2009, 4, 476-487.	1.4	1
174	Characterization of Gun Plasma Penetrated Into a Steady State Plasma Device. IEEE Transactions on Plasma Science, 2013, 41, 3122-3128.	1.3	1
175	Influence of Deuterium Retention on Secondary Electron Emission from Graphite under Deuterium Plasma Exposure. Plasma and Fusion Research, 2015, 10, 1402009-1402009.	0.7	1
176	Correlation Analysis of 3–4 Kilohertz Core and Edge Density Fluctuations in the GAMMA 10 Tandem Mirror Device. Fusion Science and Technology, 2015, 68, 125-129.	1.1	1
177	Field electron emission from metal surfaces irradiated with helium plasmas. , 2016, , .		1
178	Ignition and Sustainment of Arcing on Nanostructured Tungsten under Plasma Exposure. , 2018, , .		1
179	Characterization of He Induced Nanostructures Using SEM Image Analysis <sup> </sup> . Plasma and Fusion Research, 2019, 14, 3402049-3402049.	0.7	1
180	Evaluation of axial decay length of plasma pressure in detached plasma. Nuclear Materials and Energy, 2020, 25, 100812.	1.3	1

#	Article	IF	CITATIONS
181	Thermal treatment of W large-scale fiberform nanostructures. Physica Scripta, 2021, 96, 094004.	2.5	1
182	Comparison of Hydrogen Adsorption on Diamond and Graphite Surfaces. Plasma and Fusion Research, 2010, 5, S2072-S2072.	0.7	1
183	Superimposition of Pulses to Steady Arc Discharge in Toroidal Divertor Simulator. Plasma and Fusion Research, 2012, 7, 1405100-1405100.	0.7	1
184	Increased Energy Absorption into W due to the Metal Deposited Layer from an ELM-like Pulsed Plasma. Plasma and Fusion Research, 2019, 14, 1401051-1401051.	0.7	1
185	Plasma Potential Measurement in Detached Plasmas by Emissive Probe Considering Space-Charge-Limited Effect. Plasma and Fusion Research, 2020, 15, 1301082-1301082.	0.7	1
186	An approach to implement a heat flux limit in a model for fusion relevant plasmas. Physics of Plasmas, 2022, 29, .	1.9	1
187	Simulation on Structure and Dynamic Behavior of Dust Particles in a Direct Current Plasma-Sheath. Journal of Plasma and Fusion Research, 1999, 75-CD, 234-257.	0.4	0
188	Proposal of Flexible Atomic and Molecular Process Management for Monte Carlo Impurity Transport Code Based on Object Oriented Method. Contributions To Plasma Physics, 2002, 42, 157-162.	1.1	0
189	Formation and Dynamics of Very Deep Negative Potential Well in the Small Tokamak Device CSTN-IV. European Physical Journal D, 2003, 53, 895-902.	0.4	0
190	Three-dimensional microscopic analysis of inter-laminar area in cross-ply laminate using a homogenization theory. , 0, , .		0
191	Deuterium Uptake in Iron Oxide (Fe[sub 2]O[sub 3]) Under D[sub 2]+]-Plasma Exposure. , 2011, , .		0
192	Influence of the Probe Electrode on Probe Measurements for Atmospheric Pressure Microwave Plasma Torch. Contributions To Plasma Physics, 2013, 53, 81-85.	1.1	0
193	Compact and high-particle-flux thermal-lithium-beam probe system for measurement of two-dimensional electron density profile. Review of Scientific Instruments, 2014, 85, 093510.	1.3	0
194	Effect of nanostructured layer thickness on tungsten surface on cathode spots dynamics. , 2016, , .		0
195	Measurement of Poloidal Flow Profiles Using a Mach Probe Array in HYBTOK-II Tokamak with RMP Fields. Plasma and Fusion Research, 2017, 12, 1202027-1202027.	0.7	0
196	Morphology Changes of Platinum and Tungsten Carbide by He Plasma Irradiation. Plasma and Fusion Research, 2018, 13, 3406074-3406074.	0.7	0
197	Emission from Tungsten Nanostructured Tendril Bundles under Local Thermal Load. , 2018, , .		0
198	First EMC3â€EIRENE modelling of JTâ€60SA edge plasmas with/without resonant magnetic perturbation field. Contributions To Plasma Physics, 2020, 60, e201900114.	1.1	0

#	Article	IF	CITATIONS
199	Doppler and Stark Broadenings of He II Emission in NAGDIS-PG. Plasma and Fusion Research, 2021, 16, 1202013-1202013.	0.7	0
200	OS20-2-4 Warpage of Si/Solder/OFHC-Cu Layered Structures Subjected to Cyclic Thermal Loading. The Abstracts of ATEM International Conference on Advanced Technology in Experimental Mechanics Asian Conference on Experimental Mechanics, 2011, 2011.10, _OS20-2-4	0.0	0
201	Effect of Externally Applied Resonance Magnetic Perturbation on Current Decay during Tokamak Disruption. Plasma and Fusion Research, 2012, 7, 1202049-1202049.	0.7	0
202	Various Phenomena on PSI. PSI in Fusion Devices. Edge Plasma Physics and Atomic-Molecular Processes Journal of Plasma and Fusion Research, 1999, 75, 378-383.	0.4	0
203	Overheating of Nanostructured Tendril Bundles due to Thermo-Field Emission. , 2021, , .		0
204	Nitrogen Atom Density Measurements in NAGDIS-T Using Vacuum Ultraviolet Absorption Spectroscopy. Plasma and Fusion Research, 2022, 17, 1201004-1201004.	0.7	0
205	Isotope Effect for Plasma Detachment in Helium and Hydrogen/Deuterium Mixture Plasmas. Plasma and Fusion Research, 2022, 17, 2402027-2402027.	0.7	0